

A SWITCHED KALMAN FILTER DEDICATED TO ASSISTED PRESSURE FOOD THAWING

L. BOILLEREAUX¹, H. FIBRIANTO² AND J.M. FLAUS²

1- GEPEA, Laboratoire de Génie des Procédés, Environnement, Agroalimentaire, UMR MA 100, ENITIAA, rue de la Géraudière, BP 82225 – 44322 Nantes cedex 3

2- LAG, Laboratoire d'Automatique de Grenoble, UMR CNRS 5528, ENSIEG, rue de la Houille Blanche, BP 46 – 38402 Saint Martin d'Hères cedex

Abstract: Foodstuffs thawing under the effect of high pressure is an innovative technique allowing to increase considerably the dynamic of the process, and to limit the food damages after treatment by controlling the kinetic of the ice to water change. It is however necessary to estimate this kinetic. The methodology proposed here is a Kalman Filter applied on a switched linear hybrid system, representing the heat transfer during the three phases of water: solid, melting and liquid. This technique is carried out during the experimental thawing of a food gelatin.

Keywords : Switched Linear systems, Kalman Filter, Thawing, High Pressure

1. INTRODUCTION

High pressure assisted thawing is an emerging technology allowing to increase the kinetic of water phase change by lowering the ice/water melting point. For the moment, this technique is uniquely studied at the laboratory scale, but thanks to its numerous advantages, its industrialization will certainly be applied, as soon as the last technological constraints will be suppressed. Some advantages are the reduction of drip losses and a least quality damage, comparatively to the conventional methodologies, as Chevalier, *et al.* (1999) have proved, but the most attractive interest is certainly the reduction of the processing time coupled to a microorganism destruction. In fact, the thawing time of a food product is, under 200 MPa, only about 15% of the time needed by a classical approach (Chourot, *et al.*, 1997).

From a control point of view, the control of the applied pressure permits to master the kinetic of the thawing front inside the food product, and can be an important quality parameter to obtain an homogeneous product after treatment. In order to control the kinetic, it is necessary to know the temperature evolution inside the product. To achieve this objective, a modified Kalman filter is proposed to estimate the temperature of a food gelatin during high pressure thawing.

2. HIGH PRESSURE THAWING PRINCIPLE

Usually, the thawing operation is realized without any control variable. The ambient temperature is limited by microbiological considerations (from +4 to +10°C), with forced or natural convection. The mean value of the melting temperature of a foodstuff, under atmospheric pressure, is about of 0°C, equivalent to the water phase change temperature, its major component.

With such a small temperature difference between ambience and food, the thawing time is necessary long.

The high pressure process consists in packaging the foodstuff and placing it in a high pressure vessel filled with the pressure media, oil or water. When an isostatic pressure is applied, the water melting temperature decreases until reaching about -20°C under 200 MPa (Fletcher, 1970) ; its evolution can be computed by solving thermodynamic equations (Chizhov and Nagornov, 1991) or by using the following polynomial, established by Bridgman (1911) :

$$T_m = -0.072192 v - 0.000155 v^2 \quad (1)$$

where T_m is the melting temperature ($^{\circ}\text{C}$) and v the pressure (MPa). The temperature gradient between ambience and melting front is considerably increased, allowing to decrease the thawing time.

3. HIGH PRESSURE THAWING MODELED BY SWITCHED LINEAR SYSTEM

Concerning the modeling of this process, a solution has been proposed by Chourot, *et al.* (1997), based on finite volumes scheme, by considering a constant high pressure. Boillereaux, *et al.* (1999) have adapted the classical Plank model to design a non linear trajectory control of the thawing front, but with the restriction that the foodstuff must be initially close to the melting temperature.

However, a continuous variation is difficult to implement on such a process, due mainly to the split-range technology used. For this reason, we propose here to consider that the pressure can be controlled at a finite number of levels, between the atmospheric one and 200 MPa, and to model the temperature evolution in the foodstuff during a thawing with pressure steps. This modeling is realized in two steps presented in the sequel.

3.1 under constant pressure

Consider a cylindrical foodstuff, where the heat transfer can be considered as mono-directional and radial (symmetry of revolution and height \gg radius). To simplify the model design, the heat transfer at the surface is a contact one, with a negligible resistance. The cylinder can be split in a finite numbers of identical volumes, n , as indicated on (Figure 1).

The water contained in each homogeneous volume can be either solid, liquid or melting. In solid or liquid phases, its temperature evolves following the classical heat equation, and its mass share of ice (ice / total water ratio) is constant (respectively equal to 1 or 0). In melting phase, the temperature is constant and the mass share of ice evolves from 1 to 0.

Fibrianto (2001) has shown, that, by considering all the volumes, the model is also represented by equations (2) and (3).

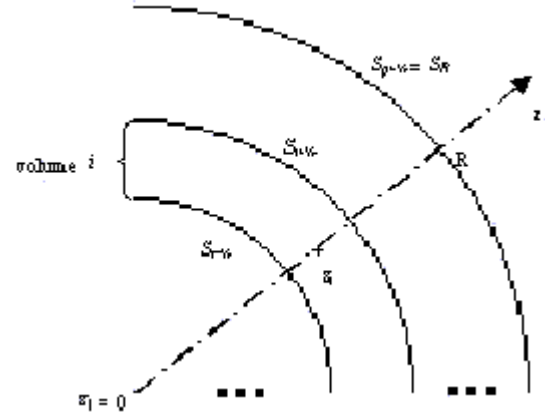


Fig. 1. Spatial mesh of the cylinder

$$\frac{dx}{dt} = (a_{ice}(v)F_1 + a_{water}(v)F_2)(Ax + Bu) \quad (2)$$

$$\frac{dz}{dt} = (Id - F_1 - F_2)(Ex + Gu) \quad (3)$$

$$E = -\frac{I(v)}{rL(v)}A \quad (4)$$

$$G = -\frac{I(v)}{r(v)L(v)}B$$

where x and z are respectively the temperature and mass share of ice vectors (n), and u the contact temperature.

λ , ρ and L are respectively the thermal conductivity, density and latent heat of the mix water/ice, and a represents either the water or the ice diffusivity.

All the thermal properties dependencies with pressure can be consulted in (Bridgman, 1911).

A is a three-diagonal matrix obtained from energy assessment applied on each volume. All the coefficients of the diagonal, upper and lower diagonals are non null, and B is a vector of zeros except the last line (see Chourot, *et al.*, 1997, for more details).

F_1 and F_2 are diagonal flag matrices, depending on the water phase in each volume, as shown in equation (5).

$$\left. \begin{array}{l} F_1(i, i) = 1 \\ F_2(i, i) = 0 \end{array} \right\} i^{th} \text{ volume in solid state}$$

$$\left. \begin{array}{l} F_1(i, i) = 0 \\ F_2(i, i) = 1 \end{array} \right\} i^{th} \text{ volume in liquid state} \quad (5)$$

$$\left. \begin{array}{l} F_1(i, i) = 0 \\ F_2(i, i) = 0 \end{array} \right\} i^{th} \text{ volume in melting state}$$

The commutations of the flags are depending on the state vector evolution, as follows:

$$F_1(i, i) \begin{cases} 1 \rightarrow 0 \text{ if } x_i = T_m \text{ and } \dot{x}_i > 0 \\ 0 \rightarrow 1 \text{ if } z_i = 1 \text{ and } \dot{z}_i > 0 \end{cases} \quad \forall i \in [1, n] \quad (6)$$

$$F_2(i, i) \begin{cases} 1 \rightarrow 0 \text{ if } x_i = T_m \text{ and } \dot{x}_i < 0 \\ 0 \rightarrow 1 \text{ if } z_i = 0 \text{ and } \dot{z}_i < 0 \end{cases}$$

3.2 With pressure steps

When a pressure step occurs, it appears in (6) that the model parameters vary. Moreover, depending on the state vector values and on the pressure step, some discontinuities in the state vector can happen. More details, concerning the discontinuities, can be consulted in (Chizhov and Nagornov, 1991). To simplify the approach, we consider that the pressure steps are sufficiently small to assume adiabatic conditions during commutations, and to neglect mass share of ice discontinuities. In other words, only the temperature sub-vector will be modified by the pressure step.

The temperature discontinuities can be taken into account in model (1), as illustrated in equations (7) and (8).

$$\dot{x}(t) = (1 - \mathbf{z}^2) (a_{ice}(v)F_1 + a_{water}(v)F_2) (Ax + Bu) + \mathbf{d}(t - \mathbf{t}) \cdot \mathbf{z}^2 \cdot \Delta x \quad (7)$$

$$\mathbf{z} = \text{sign}(\Delta v) \quad (8)$$

where δ is the Dirac function, τ the pressure step time, and v the pressure.

It means that, at any time $t \neq \mathbf{t}$, the model is (5), and at $t = \mathbf{t}$, the model is (9).

$$\dot{x}(t) = \mathbf{d}(t - \mathbf{t}) \cdot \Delta x \quad (9)$$

Due to the property of the Dirac function, the state vector at time τ is immediately deduced (10).

$$x(\mathbf{t}) = \Delta x \quad (10)$$

Δx is computed such as the value of the temperature after switching is either equal to the melting one, denoted T_m , or unchanged, depending on the operating conditions:

$$\Delta x = \left(F_1 \cdot \frac{1-w}{2} + F_2 \cdot \frac{1+w}{2} \right) (x - T_m^+) + T_m^+ \quad (11)$$

$$w = \text{sign}(x - T_m^+)$$

$$T_m^+ = T_m(v + \Delta v)$$

Let us examine equation (11). The temperature of a volume is unchanged in the case of

- the volume is thawed and its temperature is above the new melting one after pressure step.
- the volume is frozen and its temperature is below the new melting one after pressure step.

In all the other cases, its temperature is equal to the new melting one. However, due to the switching conditions proposed in (6), and to the adiabatic hypothesis, the flag matrices are unchanged.

3.3 Model validation

The model (7) has been validated during the thawing of a food gelatin cylinder (radius 5 cm, height 40 cm) in a cylinder of copper. 20 homogeneous volumes has been considered, and 9 pressure steps occurred during the experiment. In such an experiment, it is difficult to know perfectly the contact resistance between the copper and the surface of food. For this reason, the interface temperature was measured and used as input u of the system. Figure 2 presents the modeled (dotted line) and measured (continuous line) temperature at 3 different radial positions, where discontinuities due to pressure steps can be noticed.

4. KALMAN FILTER DESIGN

4.1 Observability

The model described by equations (2) and (3) is composed of two sub-vectors, denoted x and z . It can be verified that

$$\begin{cases} \frac{\partial x_i}{\partial z_j} = 0 \\ \frac{\partial z_i}{\partial z_j} = 0 \end{cases} \quad \forall i, \forall j \quad (12)$$

The first and second equalities in (12) prove that a measurement of z does not permit to estimate x and z , and the second equality prove that the measurement of x does not permit to estimate z .

In other words, it is useless to measure mass shares of ice, and their estimations are impossible from the temperature measurements.

Although the system is unobservable, it is possible to estimate the state of the water -solid, liquid or melting- and the temperature in each volume.

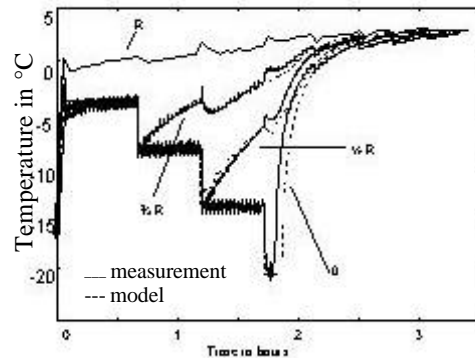


Fig. 2. Experimental validation of the model.

However, the lack of information about z prevents from estimating correctly the phase commutations, from melting to solid / liquid phases.

This estimation can be effected with a reduced number of temperature sensors, and the observer is reduced to the x sub-vector.

(Fibrianto, 2001, Boillereaux et al., 2002) have shown that two thermocouples are sufficient to reach our objective, one at the center of the cylinder, and the other at the peripheral volume. The output model can be represented by (13).

$$y = Cx \quad (13)$$

$$C = \begin{bmatrix} 1 & 0 & \dots & 0 & 0 \\ 0 & 0 & \dots & 0 & 1 \end{bmatrix}$$

With such a model, it can be verified (Boillereaux et al., 2002) that the observability matrix is always of full rank if at the most one volume is in the melting phase.

Such an hypothesis can be easily verified: due to the switching conditions (6), even if a volume reach (after a pressure step for example) the melting temperature, it cannot commute if at least one of its neighbors is already in the melting area.

The proofs of observability can be consulted in (Fibrianto, 2001).

At last, it can be verified that a pressure step do not affect the model structure, but provokes discontinuity of the state vector. Such discontinuities can be considered as disturbances, but do not constitute a brake to the observer design.

4.2 Observer design - Constant pressure

We propose here to adapt the classical Kalman filter to our switched linear system (equations 14 to 18).

$$\frac{d\hat{x}}{dt} = \hat{F} \cdot (A\hat{x} + Bu + K(t)(y - C\hat{x})) \quad (14)$$

$$\hat{F} = a_{ice}(v) \cdot \hat{F}_1 + a_{water}(v) \cdot \hat{F}_2 \quad (15)$$

$$\frac{d\hat{z}}{dt} = (Id - \hat{F}_1 - \hat{F}_2)(E\hat{x} + Gu) \quad (16)$$

$$\dot{P} = \hat{F}(AP + PA^T) + Q - KRK^T \quad (17)$$

$$K(t) = P(t)C^T R^{-1} \quad (18)$$

where P is the estimation covariance matrix, Q and R respectively the covariance matrices of the state and output noises.

The correction is effected only on the observable sub-system. In other words, the mass share of ice sub-vector is only simulated from the estimated temperature. A perfect knowledge of its initial value is crucial in this problem.

4.3 Convergence discuss

If the Kalman Filter restricted to equations (14), (17) and (18) is considered, its convergence can be proved if and only if the conditions (19) are verified.

$$\forall t, \begin{cases} F_1 = \hat{F}_1 \\ F_2 = \hat{F}_2 \end{cases} \quad (19)$$

It means that the commutations of the system and of the observers must be perfectly synchronized, in other words, the Kalman filter must have converged before the first switching. Such a condition can be envisaged, because the dynamic of the process is sufficiently slow and the initial conditions usually well-known.

Let us exam now the case of a delay between the system and observer commutation. Due to the switching conditions, only a single volume can be in the melting phase. In other words, the error concerns only two consecutive coefficients of the flag matrices. However, the convergence proof cannot be established in this case.

4.4 Observer extension – Variable pressure

By extending the previous discussion, it can be assumed that the convergence is such that the estimation error is negligible before a pressure step. Thus, the discontinuities can be introduced in the Kalman filter with a limited error, by modifying equation (14) as follows:

$$\frac{d\hat{x}}{dt} = (1 - z^2) \hat{F} (A\hat{x} + Bu + K(t)(y - C\hat{x})) + z^2 \cdot d(t-t) \cdot \Delta\hat{x} \quad (20)$$

5. EXPERIMENTAL VALIDATION

5.1 Experimental conditions

The data obtained during the model validation presented in section (3.3) has been used here off line. We have compared the application of two different Kalman filters, one based on a model with 10 volumes, and the other with 20 volumes. In both cases, the considered input u is here the ambient temperature, assumed to be constant and equal to 3°C. In fact, we have here considered that the interface copper / food resistance is negligible, and a global exchange coefficient (convection and thermal resistance of the copper) about equal to 100 Wm².

For each system, the output vector is composed of the measurement of the temperature in the center of the cylinder, and a measurement obtained from a thermocouple located about 1 mm under the surface.

With a small location error, we have also considered that this measurement corresponds for each system respectively to volume 10 and volume 20. The output model mentioned in equation (13) is also verified.

All the state variables of \hat{x} and \hat{z} are initialized respectively at -20°C and 1 kg/kg .

The whole temperature state vector is estimated, but only the estimated temperatures corresponding to the available thermocouples are presented:

$r = 0, r = \frac{1}{2}R, r = \frac{3}{4}R$ and $r \approx R$

5.2 Results and discussion

Figures 3 and 4 illustrate the estimated (dotted line) and measured (continuous line) temperatures at these 4 locations, respectively with $x \in \mathbb{R}^{10}$ and $x \in \mathbb{R}^{20}$.

It can be noticed that the number of state variables do not improve the estimation result in this case. In fact, even if the model is more precise with a fine spatial mesh, the large dimension of the state vector provokes a decreasing of the estimation accuracy.

However, the estimation error is mainly remarkable for the location $r = \frac{1}{2}R$ with $x \in \mathbb{R}^{20}$: the difference between estimation and measurement, due to the delay between the commutations from Melting to Liquid phases, as indicated on figure 4, is increased by the pressure step occurring at this time. After this period, it can be verified that the estimation converges to the real value.

REFERENCES

Boillereaux, L., J.M. Chourot and M. Havet (1999). Nonlinear trajectory control of high pressure thawing, *Journal of Process Control*, **9(4)**, 351-356

Boillereaux, L., H. Fibrianto and J.M. Flaus (2002). Switched linear modelling approach for high pressure thawing process analysis, *accepted for publication in Special Issue of International Journal of Control*

Bridgman, P.W. (1911). Water in the liquid and five solid forms under pressure, *Proc. Amer. Acad. Arts Sc.*, 441-558

Chevalier, D., A. Le Bail and J.M. Chourot (1999). High pressure thawing of fish (whiting): influence of the process parameters on drip losses. *Lebensmittel-Wissenschaft und Technologie*, **32**, 25-31

Chizhov, V.E. and O.V. Nagornov (1991). Thermodynamic properties of ice, water and their mixture under high pressure, *Glaciers-Ocean-Atmosphere Interactions IAHS Publ. no.208*, 463-470.

Chourot, J.M., L. Boillereaux, M. Havet and A. Le Bail (1997). Numerical modeling of high pressure thawing: application to water thawing. *Journal of Food Engineering.*, **34**, 63-75.

Fibrianto, H (2001). Contribution à la commande du procédé de décongélation haute pression: approches classiques et approche hybride. *Thesis of the Institut National Polytechnique de Grenoble*, to appear.

Fibrianto, H., L. Boillereaux and J.M. Flaus (2001). High pressure assisted thawing and freezing modeled by hybrid automata. *Journal of Process Control*, in revision.

Fletcher, N. H..1970 "The chemical physics of ice", *Cambridge at the University press*, pp. 50-146.

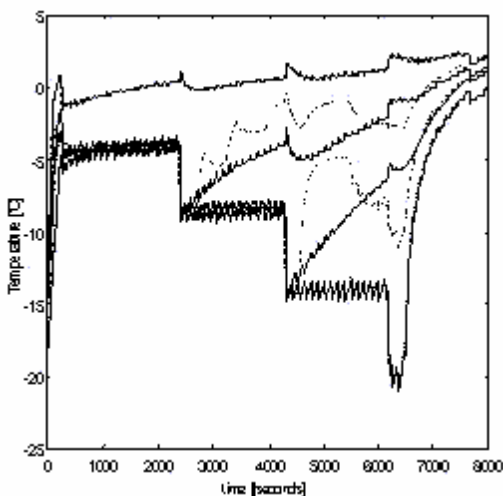


Fig. 3. Estimated and measured temperature with a 10 volumes based Kalman Filter

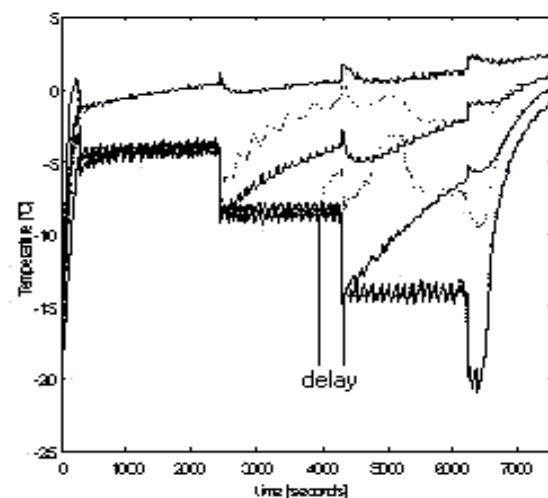


Fig. 4. Estimated and measured temperature with a 20 volumes based Kalman Filter